Influences of Metal Oxide Identity and Surface Chemistry on Ionic Conduction in Nanoparticle-Supported Ionogels

An Honors Thesis for

The Department of Chemical and Biological Engineering

By

Jerren Grimes

Tufts University 2015

Acknowledgements

This thesis was made possible via the esteemed contributions of various individuals and organizations. I am exceptionally grateful to Professor Matthew Panzer for his patience, encouragement and expert advice, which has been instrumental not only in the success of this thesis but also in my personal development as a researcher. I am also indebted to him for allowing me liberal use of the Green Energy and Nanostructured Electronics (GENE) Laboratory. I would also like to thank several members of the GENE Lab group including Changqiong Zhu for her assistance with SEM imaging, Ariel Horowitz for her guidance on safely working with nanoparticles and Adam Visentin for his instruction on synthesizing gel electrolytes. I would like to especially acknowledge Anthony D'Angelo for his mentorship, advice and instruction throughout my various scientific endeavors.

I must also extend my gratitude to The Office of the Provost and other individuals responsible for the sponsorship and successful running of the Summer Scholars program within which this research began. I would also like to express my appreciation to Evonik Industries for their generous donation of various metal oxide nanoparticles. I am also appreciative of the feedback Professor Charles Sykes of the Chemistry Department has provided in the development of this research.

Finally, I am particularly thankful for my engineering colleagues and friends for their encouragement and counseling and my family for their continued support in all of my undertakings and inspiring me to strive for excellence.

Table of Contents

List of Figures

List of Tables

Abstract

Ionogels are a new class of solid electrolyte material that has been proposed as a viable replacement to conventional electrolytes used in batteries and supercapacitors. The electrostatic characterization of ionogels based on metal oxide nanoparticles have not been explored in depth however and this knowledge would be key to making informed decisions about material choices for device fabrication. This research involves the synthesis of novel ionogels based on three different metal oxide nanoparticle species with either hydrophilic or hydrophobic surface characteristics with the goal of analyzing the interactions, if any, between the surface of the particles and the ions of the ionic liquid. The nature of gelation was found to be a strong function of particle size and the particle hydrophobicity. Contact angle measurements suggest that the hydrophobic EMI TFSI ionic liquid more readily wets a hydrophilic surface (contact angle of 10.1˚) compared to a hydrophobic surface (contact angle of 59.5˚). Activation energy of the ionic conductivity, which is a descriptor of the barrier the ions in a gel experiences under a potential difference, was found to be a function of surface chemistry and oxide identity with gels made using hydrophilic particles having a higher E_a than their hydrophobic counterparts. For all of the samples however, activation energy only ranged between 14 and 16 kJ/mol implying that nanoparticle based gels are suitable for minimizing scaffold-ion interactions. Ionic conduction for hydrophilic gels was also slightly less than that for hydrophobic ones. The electrostatic trends observed could be explained by the additional presence of hydrogen bonding between the ions and scaffold in hydrophilic gels.

1. Introduction

1.1. Overview

Advances in computer hardware and manufacturing techniques have enabled a massive reduction in the size of and energy required by computer chips. Despite significant advancements in the field however, battery technologies have not been able to keep up with rapid advancement associated with semiconductor computer hardware in the last fifty years [1]. Energy storage devices like batteries and supercapacitors have been limited primarily by the availability and existence of different electrochemical materials. In particular, the liquid electrolyte in these devices can be improved. Conventional electrolytes have been a cause for concern since they can leak and therefore they must be especially encapsulated, leading to higher costs of manufacturing, heavy, bulky batteries and a smaller volume available for useful material. There is also a flammability hazard associated with the liquid electrolytes used today.

Ionogels are a new class of solid electrolyte material with enormous promise for use in energy storage devices such as batteries and supercapacitors [2]. Typically, an ionogel is comprised of an ionic liquid immobilized in a solid scaffold material. An ionic liquid can be defined as a salt, much like common table salt, that is a liquid at room temperature. Ionic liquids are unique however, in the sense that they have high ionic conductivity and can operate within a high electrochemical potential window compared to aqueous electrolytes [2]. In addition, the liquid is thermally stable and has a negligible vapor pressure due to the presence of strong ionic bonds which results in non-volatility and non-flammability [3]. Ionic liquids have been categorized as green materials since they can be readily recovered and recycled several times using little energy and are very chemically and thermally stable [2].

An ionogel contains a solid interconnected matrix host, usually composed of polymers, organic gelators or more recently metal oxides, that constrains the ionic liquid and is able to prevent its flow [3]. Currently, ionogels are being touted as the future replacements for electrolytes within batteries and supercapacitors. This is because they still maintain the high ionic conductivity and other beneficial properties of the pure ionic liquid, despite being a solid. Gels are easier to work with, safer and provide a greater flexibility with device construction than liquids. For example, using an ionic liquid gel electrolyte in place of a liquid one means that the device does not need to be especially encapsulated to prevent leaking or evaporation.

Gels made using nanoparticle species have been recently explored and show great potential since a small amount by mass of nanoparticle is necessary for gelation so the properties of the liquid are mostly retained. For ionogels and their potential to be incorporated into energy storage devices, a greater understanding of the chemistry within the gel between the liquid and solid scaffold must be obtained so that more informed decisions can be made in the choice of materials used to fabricate such a device.

1.2. Background

Metal oxide nanoparticle supported ionogels have only recently been explored as an entirely new class of material for energy storage devices. Ueno et al provides a comprehensive study on the rheological properties of fumed silica nanoparticles in several hydrophobic and hydrophilic ionic liquids [4]. They find that the nature of the colloidal dispersion of the particle network varies depending on the surface chemistry and for example, the gels made with hydrophilic silica in hydrophobic ionic liquids exhibit a shear thinning behavior. Furthermore, gels were able to form in every case where hydrophobic silica was utilized, independent of the hydrophobicity of the ionic liquid. The ionic conductivity in silica nanoparticle supported ionogels as a function of particle concentration was also investigated and in comparison to the neat ionic liquid, a slight decrease in conductivity was observed [5]. Wittmar et al has explored the stability of colloidal structures based on differently sized titania nanoparticles in hydrophobic ionic liquids and found that the size of the particle determines the stability of the colloidal network, i.e. whether or not a gel can form [6]. While literature exists for the electrostatic characterization of ionogels as a function of different polymer scaffolds [7], an in depth look at the electrostatic properties of ionogels based on nanoparticles as a function of the particle identity and surface chemistry has yet to be performed.

In order to make better decisions about the choice of ionic liquid and scaffold material for energy storage applications, the chemical interactions between them in an ionogel may be investigated. This characterization would involve measurements of ionic conductivities and the temperature dependence of conductivity, expressed through the activation energy. This thesis therefore attempts to explore whether the surface chemistry of the scaffold material, i.e. its hydrophobicity, and the identity of the metal oxide used has any measurable effect on the ionic conductivity of the hydrophobic EMI TFSI IL and the activation energy of ionic conductivity in the gel.

1.3. Theory

When a potential difference is applied across the ionogel material, the ions that comprise the ionic liquid are set into motion, creating a current (i.e. a flow of charge over time). Previous studies have shown that the presence of the solid scaffold material can influence the flow of the ionic species, usually hindering their motion [7]. One theory is that the scaffold material obstructs the movement of ions while they are traversing the length of the gel and therefore the overall conductivity is reduced with increasing scaffold weight percent or concentration [8].

Less explored however are the chemical interactions between the scaffold surface, whether it be polymer or nanoparticle, and the ions of the ionic liquid and whether or not they are significant enough to have a macroscopic impact on ionic conductivity as compared to the neat ionic liquid conductivity. In literature, this has been quantified by the measurement of activation energy, E_a, which can be extracted from AC impedance spectroscopy data. Activation energy in the realm of chemistry has typically been thought of as the minimum energy input required for a chemical reaction to proceed. In this discussion however, activation energy is considered a descriptor of the influence the solid scaffold material has on the conductivity of the neat liquid electrolyte with higher activation energies representative of a greater hindrance to the motion of the ions under some applied voltage. AC impedance spectroscopy measures the impedance over a range of voltage frequencies of an electrostatic system. The impedance, $|Z|$, has a real and an imaginary part with the real part associated with the resistivity of the material and imaginary value associated with the reactance or capacitance. Figure 1.3.1 shows typical |Z|, vs. Frequency results of an ionogel during AC impedance spectroscopy at different temperatures.

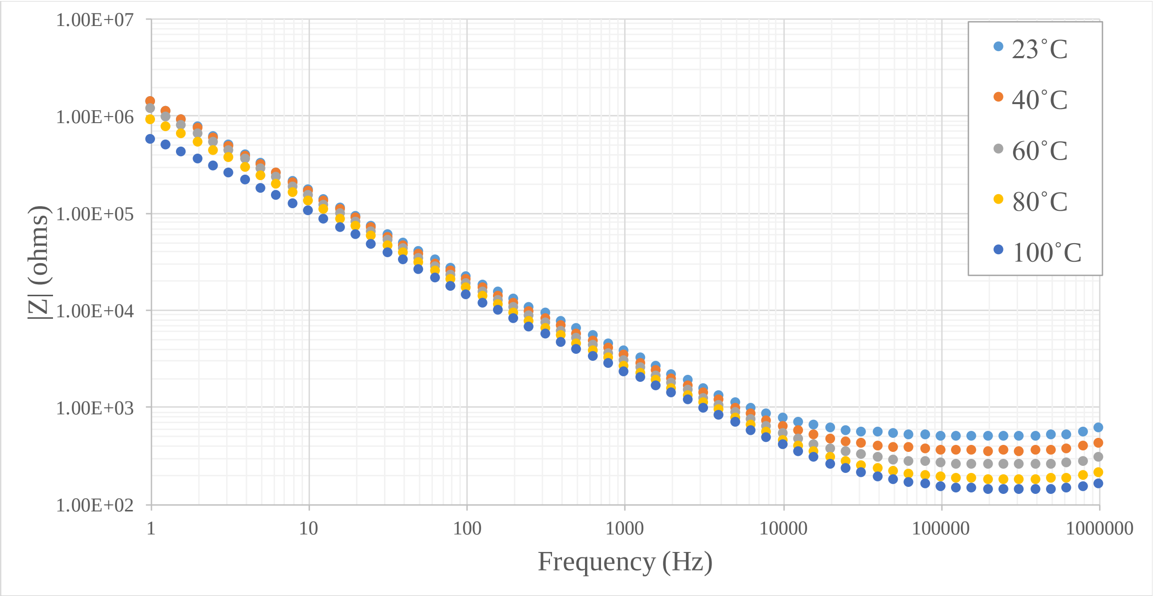

Figure 1.3.1 Impedance (|Z|) vs. Frequency from AC Impedance Spectroscopy measurements for SiO_2 at different temperatures

At very low frequencies, the sample has time to form an electric double layer around the electrodes, i.e. storing charge and therefore acting as a capacitor. At high frequencies, the sample is unable to store any significant amounts of charge because of the short time allowed and therefore it behaves as an ohmic resistor. The real value of |Z| at high frequencies can therefore be approximated as the resistance of the sample. With increasing temperature, the graph shifts down which implies a reduction in resistance within the sample. Increasing the thermal energy to this system increases the ion mobility within the gel and therefore the resistance is decreased as the ions can carry the charge in less amount of time. The conductivity of the sample is inversely proportional to the resistance measured as demonstrated by the following equation.

$$\sigma = \frac{l}{R \cdot A}$$

(E-1)

σ – conductivity (S/m)	R – resistance (Ω)
A – cross sectional area (m^2)	l – length of gel (m)

From this equation, conductivity can be easily extracted if the geometry (length and cross sectional area) is known. The Arrhenius equation shown below has typically been used to describe the dependence of conductivity with temperature.

$$\sigma = \sigma_0 \exp\left(-\frac{E_a}{RT}\right)$$

(E-2)

σ - conductivity (S/m)	σ_0 – conductivity constant (S/m)
E_a – activation energy (kJ/mol)	R – molar gas constant (8.314×10^{-3} kJ/mol)
T – temperature (K)	

It is straightforward then to extract the activation energy for a particular sample at some temperature if conductivity data is fit to equation E-2 above.

The strength of the attraction between the hydrophobic ionic liquid and the hydrophobic and hydrophilic surfaces can be estimated by contact angle measurements using a contact angle goniometer. Contact angle describes the thermodynamic equilibrium of the interfacial tensions between the solid-liquid, liquid-vapor and solid-vapor boundaries i.e., the surface wettability [9]. A small volume of the liquid is dropped on the surface of interest and a camera attached to a computer captures the outline of the drop on the surface of interest.

1.4. Objectives

The primary purpose of this investigation is to determine whether or not the hydrophobicity of the surface of a metal oxide nanoparticle and the metal oxide identity has any effect on the activation energy and ionic conductivity within an ionogel, when used as the scaffold material. To characterize the nature of the attraction between the different metal oxide surfaces and the ionic liquid EMI TFSI, contact angle measurements are made. The activation energy is determined using AC impedance spectroscopy in different volume percents and packing factors for the ionogels as E_a is a descriptor of the interactions between the ions of the ionic liquid and the solid scaffold. Room temperature ionic conductivity measurements for gels based around a common packing factor are made to determine if any trends exist.

Finally, novel metal oxide nanoparticle species for ionogel synthesis are utilized in this investigation and a secondary objective is to determine whether these particles (alumina and titania) can be successfully used to produce gels and to characterize the nature of gelation within these types of gel electrolytes.

2. Experimental Methods

2.1. Materials

The ionic liquid used in this investigation was 1-ethyl-3- methylimidazolium bis(trifluoromethylsulfonyl)imide (EMI TFSI) and its chemical structure and properties are shown in the figure and table below. The 2D molecular area was calculated based on the approximate sizes of each ion provided by Largeot et al [10].

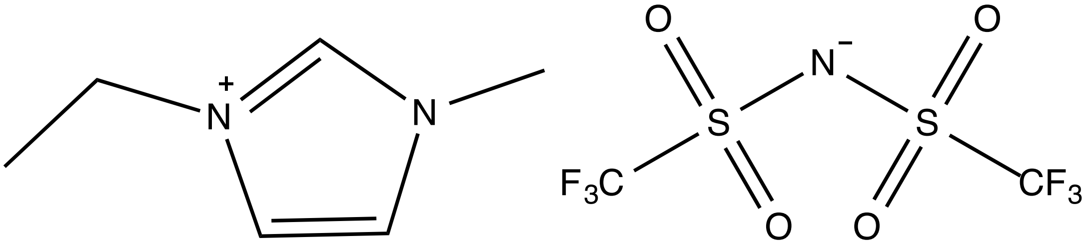

Figure 2.1.1 Chemical Structure of the ionic liquid EMI TFSI

Table 2.1.1 Properties of the ionic liquid used in this investigation

Identity	**Density (g/cm^3)**	**Molecular Weight (g/mol)**	**Approximate Molecular Area (nm^2)**
EMI TFSI	1.52	391.91	0.56

EMI TFSI is a hydrophobic and transparent ionic liquid that has been well documented and it has shown promise for use in energy storage devices due to its high electrochemical window of stability, thermal stability and high conductivity.

The solid scaffold that confines the liquid and thus creates the gel can be a wide range of materials as explained previously [3] but this investigation utilizes metal oxide nanoparticles. The nanoparticles have the advantage over other scaffolds of requiring a smaller minimum weight percent to form a gel, an extremely simple gel manufacturing process, high thermal stability and are also easy and safe to work with. Six different metal oxide nanoparticle species, which were generously donated by Evonik Industries, were used in the synthesis of EMI TFSI based ionogels. The names and compositions of these particles are summarized in Table 1.2.1 below. All species with 805 in the brand name implies an after treatment coating of trimethoxy(octyl)silane to make the particle surface hydrophobic. The metal oxides without this coating are naturally hydrophilic. The specific surface area values and densities are taken from the specification sheet that arrived with the samples and typically would vary slightly between batches. A larger specific surface area implies a smaller particle size.

Table 2.1.2 Metal oxide species and their properties

Brand Name	**Chemical Formula**	**Specific Surface Area (m^2/g)**	**Density (g/cm^3)**
Aerosil ® 200	SiO_2	216	2.20
Aerosil ® 805	SiO_2	160	2.20
Aeroxide ® Alu C	Al_2O_3	97	3.27
Aeroxide ® Alu C 805	Al_2O_3	95	2.60
Aeroxide ® TiO_2 P 25	TiO_2	35	4.1
Aeroxide ® TiO_2 T 805	TiO_2	48	3.5

2.2. Fabrication

Metal oxide nanoparticle based ionogels are synthesized using a very simple manufacturing process.

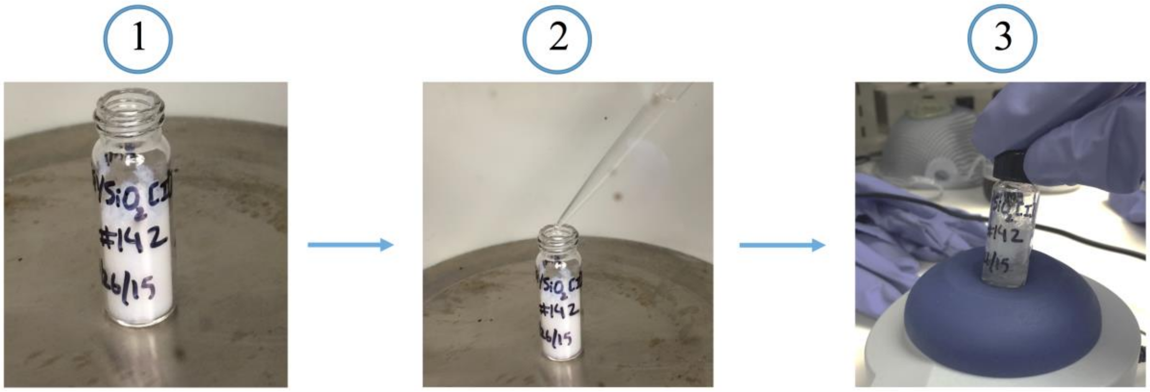

Figure 2.2.1 Synthesis process for nanoparticle based ionogels

In step 1, a predetermined mass of nanoparticle species is added to a clean glass vial using a spatula. Care should be taken when adding the nanoparticle species as the particles can easily float or bounce away while being handled. In step 2, a predetermined mass of ionic liquid (in this case EMI TFSI) is added drop wise to the vial containing the nanoparticle species. In the final step, the vial is covered and placed in a vortexer for approximately 5 minutes to allow the liquid and solid particle species to fully mix and gelate. A gel in this investigation is defined as a mixture of the ionic liquid and nanoparticle species that does not flow when inverted. The final ionogel product is shown in Figure 2.1.2 below.

Figure 2.2.2 Typical gel sample showing no flow upon vial inversion

Gel compositions are determined using several methods. Firstly, gels are fabricated based on the minimum amount of nanoparticle required for gelation, also known as the gelation point. This is done by adding a small amount of nanoparticle material to 800mg of ionic liquid and vortexing until the inverted vial no longer flows. This mass was determined as adequate to create enough sample material to twice fill the Teflon spacer used to fix a specific geometry for AC impedance spectroscopy tests. Secondly, gels are fabricated using a volume percentage of nanoparticle matter in the gel body. A desired volume percent is decided upon to compare all of the gels and then using the density values listed in Table 2.1.2, the mass of nanoparticles required to give a desired volume fraction is determined. A volume percent comparison enables a determination on whether or not the size of the particles in the gel influences the ionic conductivity. Lastly a ‘packing factor’ is used to define the gel composition and may be defined as the product of the mass of nanoparticles used and the specific surface area of the nanoparticle as provided by the manufacturer divided by the volume of the gel system (measured in μm^{-1}). A specific packing factor is agreed upon to compare all of the gels and then the desired mass to obtain this ratio is determined. The packing factor comparison is useful as it describes the approximate contact the ionic liquid has with the hydrophobic or hydrophilic surface of the particles. Each method described above can also be written in terms of weight percent of the gel, which is the mass of nanoparticle material divided by the total mass of the ionogel.

2.3. Temperature Stage Testing

A Teflon ® ring (0.3cm height and $0.44cm^2$ inner cross sectional area) with two cylindrical holes carved to exactly fit the electrode thickness in the sides is placed on a clean glass slide. This setup is placed onto the temperature-controlled plate and the needle-like electrodes are inserted into the holes. Using a spatula, the gels are scooped into the spacer cavity, making sure that it is completely filled and that the top surface is relatively flat. A schematic of this set up along with an actual test is shown in Figure 2.3.1 below.

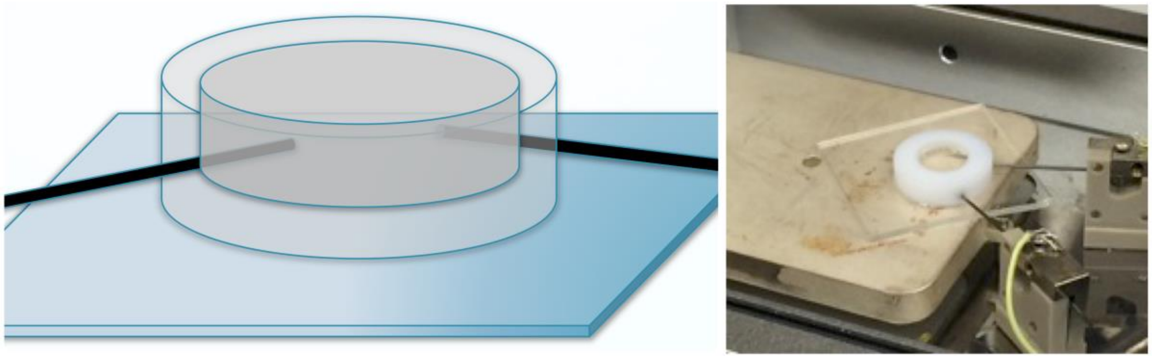

Figure 2.3.1 Schematic of Gel on Temperature Controlled Plate

The temperature of the plate was ramped up to 100˚C from room temperature (22.4˚C) over an interval of six minutes. This was done to allow the gel time to mold into place as the heating process is thought to better set the gel by removing air pockets and making proper contact with the electrodes. Then after fifteen minutes, the impedance as a function of frequency was measured using the VersaStat 4 ® potentiometer and recorded in a Microsoft Excel ® sheet. The temperature was then lowered by 10˚C and allowed to equilibrate for ten minutes before the impedance values at this new temperature was measured.

This was repeated until impedance measurements were taken between 1 and 1×10^6 Hz for the temperatures of 23˚C (room temperature), 30˚C, 40˚C, 50˚C, 60˚C, 70˚C, 80˚C, 90˚C, and 100˚C. The resistance in ohms was taken as the average impedance value at high frequencies where the graph appears horizontal (See Figure 1.3.1).

The Arrhenius Equation described in E-2 can be re-written in a more useful straight line form given by equation E-3 below.

$$\ln(\sigma) = \ln(\sigma_0) + \frac{1}{T}\left(\frac{-E_a}{R}\right)$$

(E-3)

A plot of ln (σ) versus temperature in Kelvin gives a straight line in which the activation energy, E_a, can be extracted from the slope of the line. From this equation it can be seen that it is not necessary to calculate an actual conductivity value for each temperature since only the slope of this line is important and the slope would not change if the relationship between the measured resistance and conductivity is kept constant, which in this case it is. In other words, the inverse of the resistance values determined can be substituted for the conductivity variable in equation E-3 and the slope of the line, i.e. the E_a would not change between these two possibilities as they are proportional to each other. An example of this straight line with the equation and R^2 value is provided in the figure below based on actual experimental data.

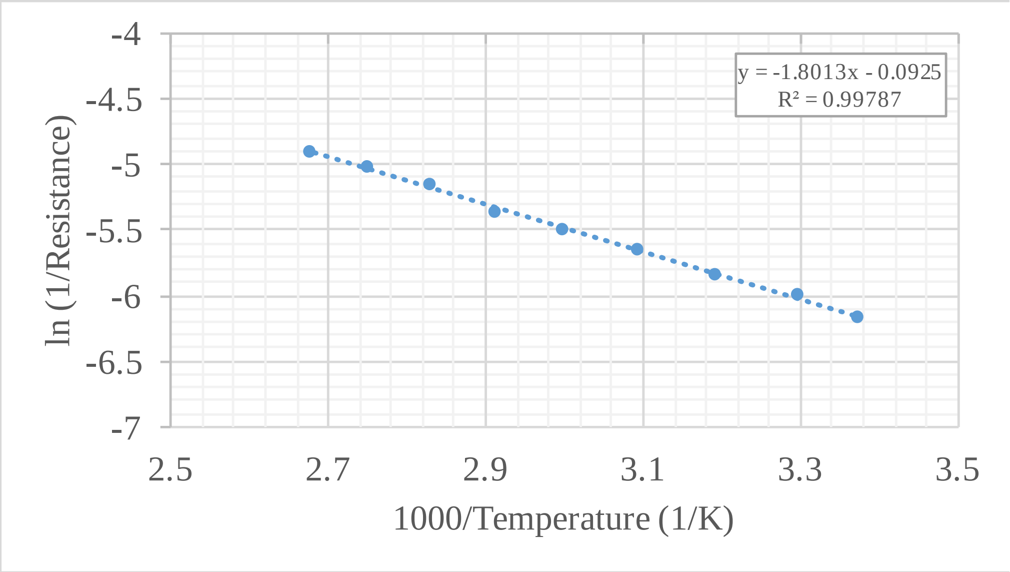

Figure 2.3.2 Arrhenius straight-line plot for hydrophilic SiO_2 at the gel point. The activation energy determined for this sample was 14.98 kJ/mol.

2.4. Contact Angle Measurements via Goniometry

For contact angle measurements, 2µl of the ionic liquid EMI TFSI was placed on either an untreated, hydrophilic or hydrophobic treated glass slide. The contact angle was measured using a ramé-hart contact angle goniometer at three different locations on the slide and then an average was determined.

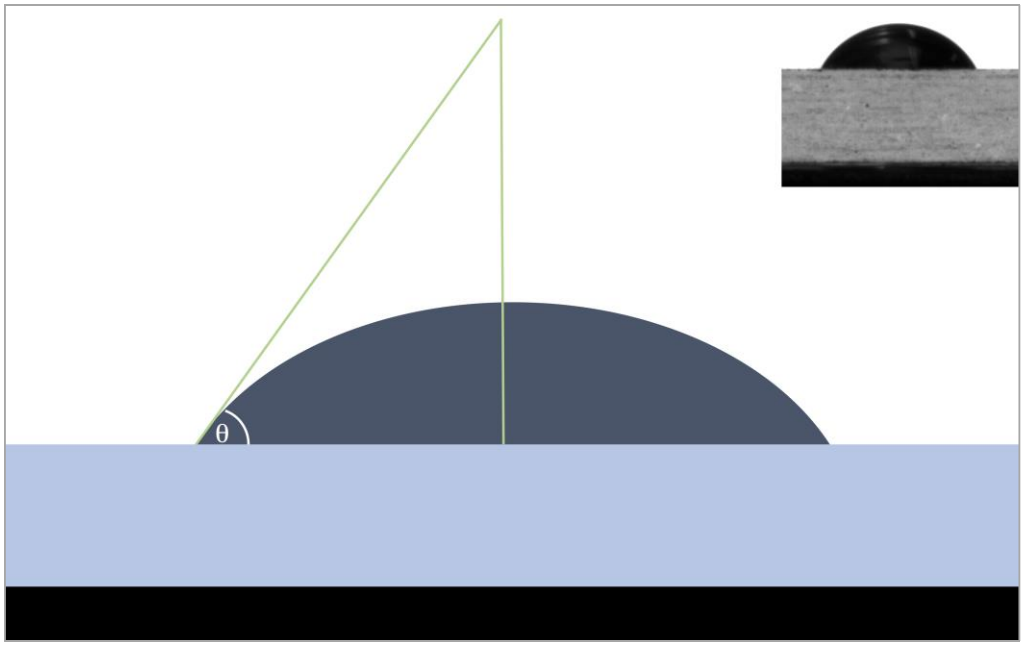

Figure 2.4.1 Schematic of a drop of a liquid on a surface of interest for measuring the contact angle. Inset shows what this may typically look like.

The computer software is able to measure the angle that the edge of the drop makes with the surface and this measurement is directly related to the surface attraction or repulsion between the liquid, air and the surface. Figure 2.4.1 shows how this typically appears on a computer screen and how the contact angle is measured. A smaller angle suggests that liquid 'likes' the surface, i.e. it is able to form strong bonds with it. To create a hydrophilic coated glass slide, a cleaned glass slide was placed in 1M NaOH solution for 30 minutes to allow the surface to be hydrolized, then immediately rinsed with deionized water and dried with a pure N_2 stream as recommended in a previous procedure [11]. To create a hydrophobic glass slide, a cleaned glass slide was first dipped in 1M NaOH solution for 30 minutes. Then, the slide was rinsed in DI water and dipped in a solution of 40mL of anhydrous toluene, 200µl of trimethoxy(octyl)silane and 1ml of concentrated HCL as recommended in a previous procedure [9]. Then, the slide was rinsed with toluene, followed by ethanol and finally deionized water. The slides were finally dried with a pure N_2 stream. For comparison, contact angle measurements were also done on an untreated clean glass slide.

2.5. Room Temperature Conductivities

A special cell testing assembly was created to perform this measurement. The height of the assembly was 0.29 cm and the spacer had a cross sectional area of 0.32 cm^2, measured with digital calipers. This set up is shown in Figure 2.5.1 on the following page.

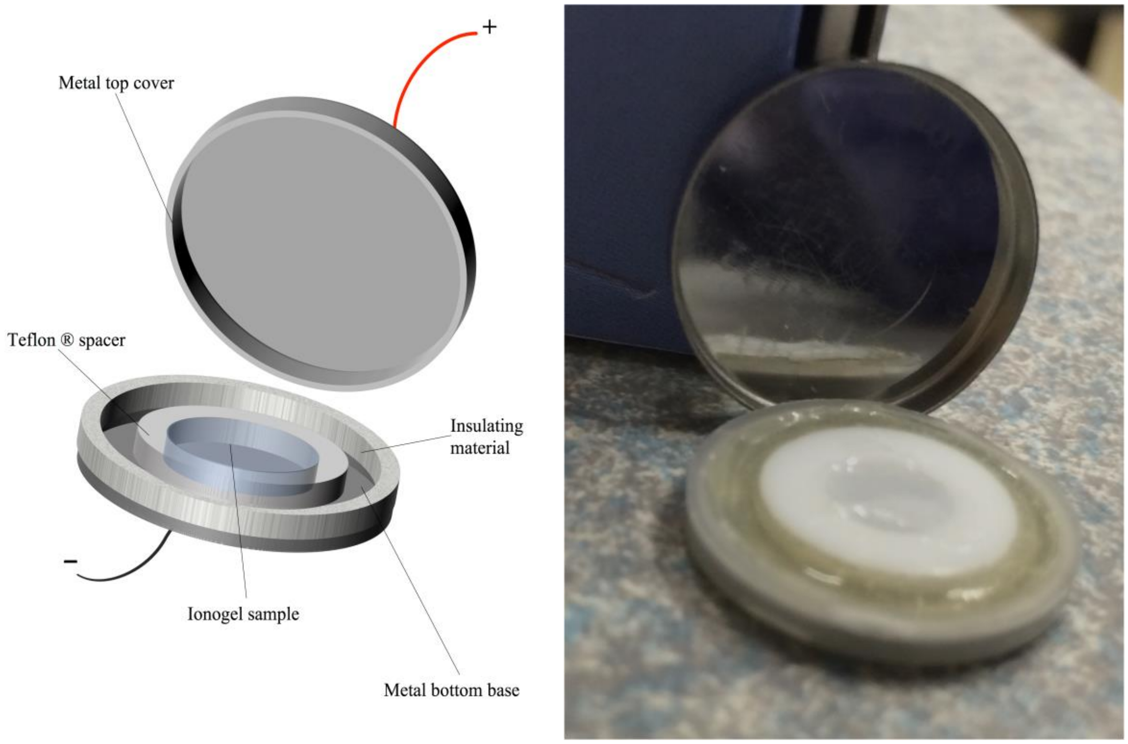

Figure 2.5.1 Cell tester assembly for measuring the room temperature ionic conductivity of the sample.

The gel sample was scooped into the spacer cavity, shaped using the spatula to be flush with the spacer surface and the cell was closed shut. This assembly was advantageous in that it allowed us to maintain the surface area contact of the electrodes with the gel sample. Using the potentiometer, the room temperature resistance was measured for the sample. From Equation E-1, the conductivity was calculated. Preliminary results suggested that there was a difference in activation energy between hydrophobic and hydrophilic species and therefore the gels tested in this experiment only compares those of similar packing factor.

3. Results and Discussion

3.1. Gel Color and Scaffold Characterization

Ionogels based on EMI TFSI were fabricated using the methodology described in section 2.2.

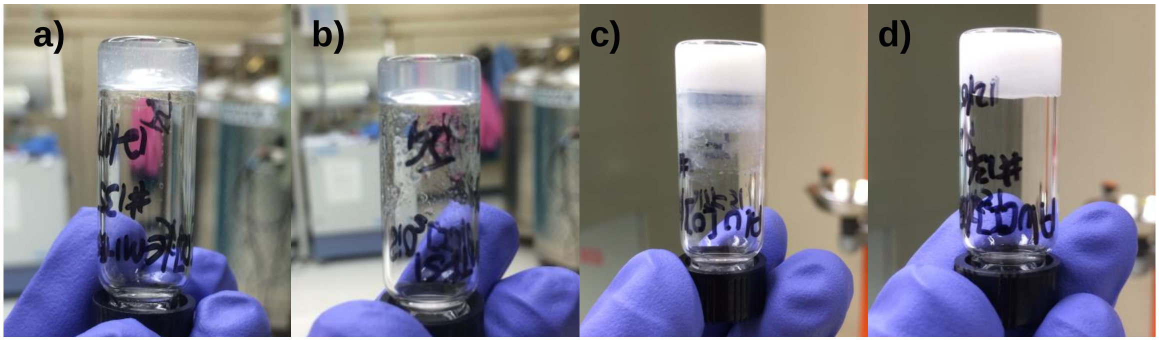

Figure 3.1.1 Ionogels based on silica and alumina nanoparticles.

a), b) – These gels are formulated using hydrophobic and hydrophilic silicon dioxide nanoparticles respectively. Gels based on silica nanoparticles have been previously demonstrated in literature [4] and have typically appeared as transparent at low weight percents (~ 3 – 5 %). This transparency is a function of the size of the nanoparticle species and suggests minimal light scattering interference.

c), d) – These gels are formulated using hydrophobic and hydrophilic coated aluminum oxide nanoparticles respectively. They appear white and are opaque in contrast to the silica-based gels. The particles within the gel network are a bit larger, as evidenced by their specific surface area, and effectively scatter all wavelengths of visible light making it appear white.

Gels were not possible with titanium oxide based nanoparticles, either hydrophilic or hydrophobic. The figure below shows the combination of hydrophilic titanium oxide and the IL showing a clear phase separation between the two. The addition of more titanium oxide did not result in a gel species.

Figure 3.1.2 Phase separation in TiO_2 based gel mixture

The nature of gelation in these ionogels comprised of nanoparticles has been examined in literature by Ueno et al but a comprehensive analysis has yet to be done [5][12]. It has been proposed that gelation is as a result of the colloidal instability of the nanoparticles in the ionic liquid, which leads to flocculation and the formation of a three-dimensional particulate network structure in a gel [4]. In fact, Ueno et al. has previously investigated the network within these types of gels to find that it exists as an expansive and loosely bounded structure of nanoparticles and gelation arises as a result of this arrangement permeating the entire continuous IL phase [12]. Van der Waals forces and electrostatic interactions are the primary sources of interparticle attractions that lead to flocculation. However, in the case of hydrophilic oxides, there is also interparticle attraction due to hydrogen bonding between the surface groups of the particle. For example, in the case of hydrophilic silicon dioxide, silanol groups on the surface can form hydrogen bonds with each other and aid in the flocculation of particles. An example of this interparticle bonding can be shown below in the figure below.

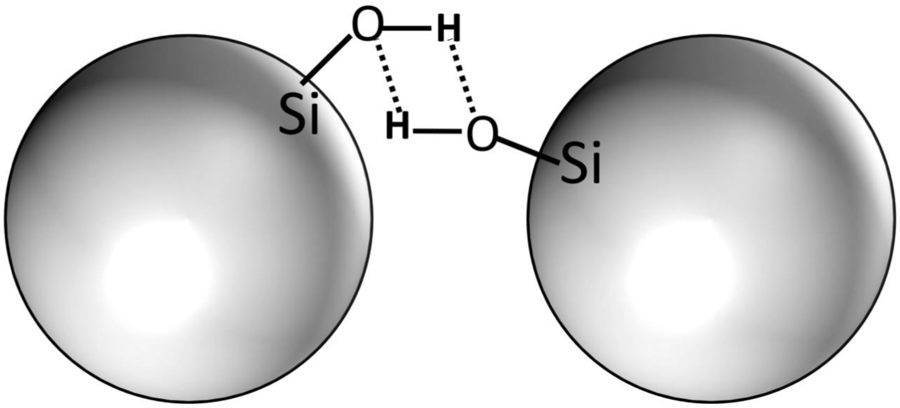

Figure 3.1.3 Hydrogen Bonding between silanol groups on the surface of hydrophilic silica

A strange observation is made upon agitating a gel sample based on hydrophilic particles in a glass vial. Upon shaking, the gel appears to form a fully liquid state and readily flows. However, after resting for a short period of time (~1 – 2 minutes), the sample assumes it's previous gel state. This experiment can be repeated several times with the same sample successfully and the time to attain a gel state once again decreases with increasing initial particle concentration in the sample. A possible explanation for this phenomenon is that the physical shaking of the vial actually disrupts the interparticle bonding, thus weakening the nanoparticle network and dismantling the gel. This observed thixotropy was more pronounced in the gels made by hydrophilic particles compared to hydrophobic ones which suggests that it is the hydrogen bonds that are being broken upon agitation.

The addition of an ionic liquid has a number of effects on the network structure within these ionogels and furthermore, the surface chemistry of the particles play a role. It has been previously demonstrated that hydrogen bonding can exist between the hydrophilic surface and the electronegative elements such as fluorine in the $TFSI^-$ anion of this particular ionic liquid [13]. This can lead to the formation of a solvation layer around the particles, which would inhibit attractive forces and help stabilize the colloidal aggregates. With a hydrophobic surface however, this effect is much less influential. This can explain the observation seen by Ueno et al that all in a series of hydrophobic ionic liquids were able to gelate with hydrophobic silica species while only some formed gels with hydrophilic silica [4]. For the ionic liquid tested in this investigation however, the surface chemistry did not appear to determine whether gelation was possible or not. Hydrophilic particles mixed more easily and quickly than hydrophobic ones but after enough time had passed on the vortexer, both gels were identical in appearance. This suggested that the hydrophilic particles had stronger interparticle interactions than the hydrophobic, most likely due to the availability of hydrogen bonding and that the presence of any hypothetical solvation layer was negligible. Contact angle measurements discussed later confirm this hypothesis.

Wittmar et al have found that the stability of colloidal networks in hydrophobic ionic liquids are a function of particle size for titania nanoparticles [6]. Larger particles are unable to form as densely packed aggregate network clusters compared to smaller ones. It is theorized then that it is more difficult to form a gel with a larger particle size. SEM images were taken of each of the six particle species provided and the appearance between hydrophobic and hydrophilic samples of the same oxide were negligible.

Furthermore, silica and alumina samples were similar in appearance under the microscope. Titania based nanoparticles were significantly larger compared to their silica and alumina oxide counterparts however. See Appendix C for all SEM images.

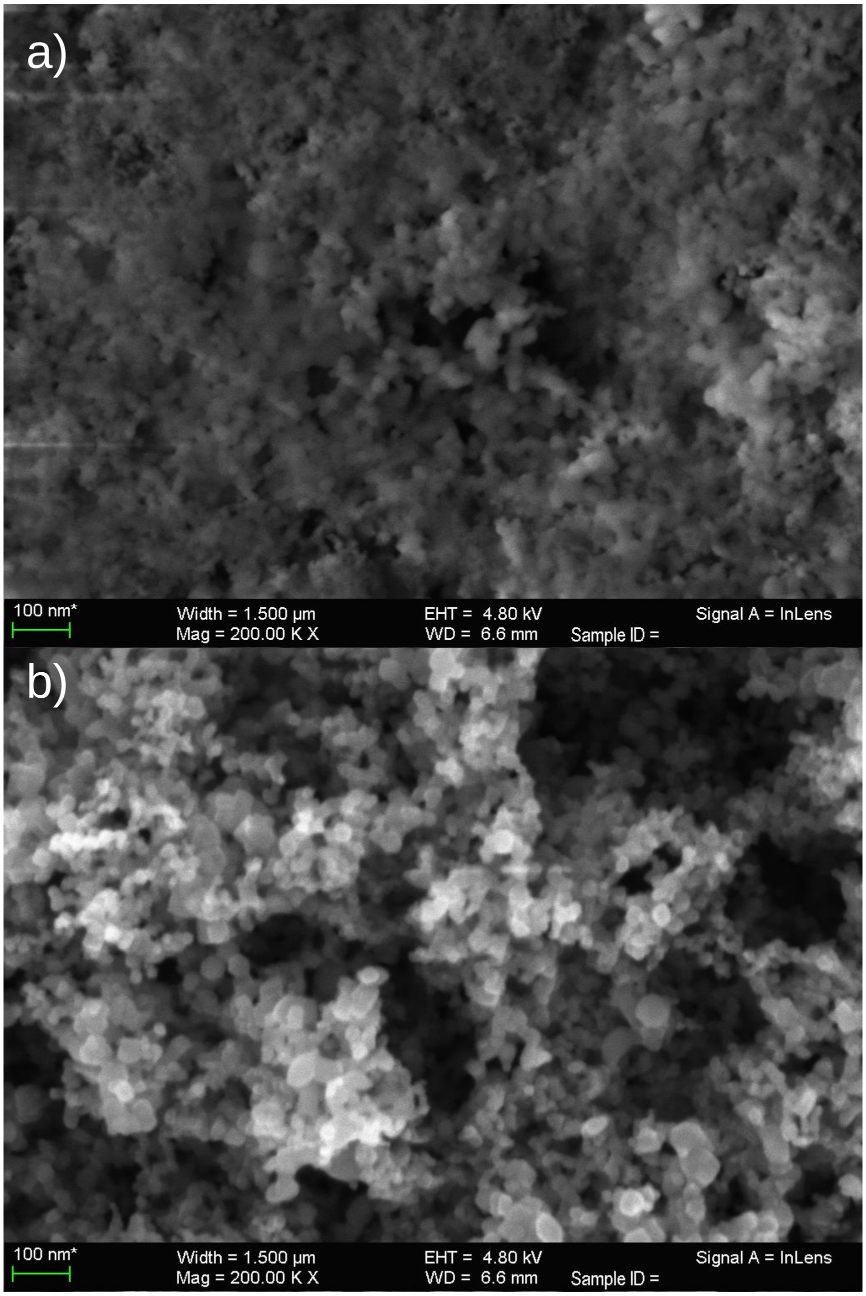

Figure 3.1.4 SEM images at 200K X of a) SiO_2 species and b) TiO_2 species

Figure a) shows the SEM image at 200 K magnification of hydrophilic SiO_2 particles while b) shows that of TiO_2 particles. The difference in size of the aggregates is significant between the two images. It is possible then that based on size alone, titanium oxide based ionogels cannot form because of the absence of the characteristic particulate network necessary to trap the ionic liquid sufficiently. The specific surface areas of titanium oxide particles are also much less, confirming that they have a larger size than the other oxides. In agreement with the literature findings, larger particles are less able to create the necessary fractal structure for a gel system [5].

3.2. Hydrophilicity and Hydrophobicity of Nanoparticles

The nanoparticles in this study are coated in the manufacturing process to make them either hydrophilic or hydrophobic. The hydrophilic silica, alumina and titania are naturally hydrophilic. The hydrophobic silica, alumina and titania are coated with trimethoxy(octyl)silane. A hydroxylated surface is present naturally on these metal oxide species. Their surface functionality may be adjusted however by a reaction with alkoxysilanes in a process known as silanization. Hydroxyl groups on the surface of the material react with trimethoxy(octyl)silane in this case as depicted by the scheme below.

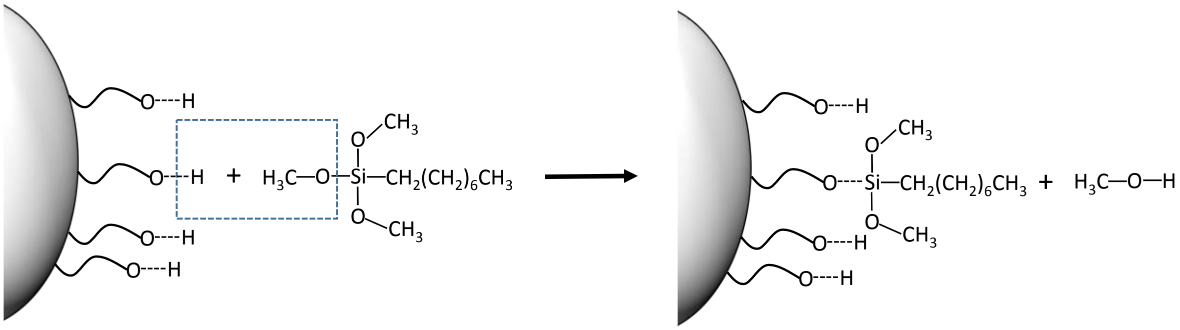

Figure 3.2.1 Silanization of hydroxyl groups on the surface of a metal oxide

To quantify the nature of the attraction between the hydrophobic EMI TFSI ionic liquid and hydrophilic and hydrophobic surfaces of the nanoparticles, a goniometer was used to measure the contact angle made between 2µl of the ionic liquid and a treated glass slide. The contact angle with an untreated glass slide is also compared. See Section 2.4 for the glass slide coating manufacturing procedure.

Table 3.2.1 Contact Angle measurements on different surfaces

	Contact Angle in Degrees		
	NaOH treated (hydrophilic)	**Untreated glass slide**	**Trimethoxy(octyl)silane treated (hydrophobic)**
Trial one average	9.7	36.8	57.8
Trial two average	9.2	36.9	59.9
Trial three average	11.4	38.1	60.9
Total Average	**10.1**	**37.3**	**59.5**

This data conforms to the results obtained in similar investigations that measured the contact angle of hydrophobic ionic liquids on treated ITO slides [14].

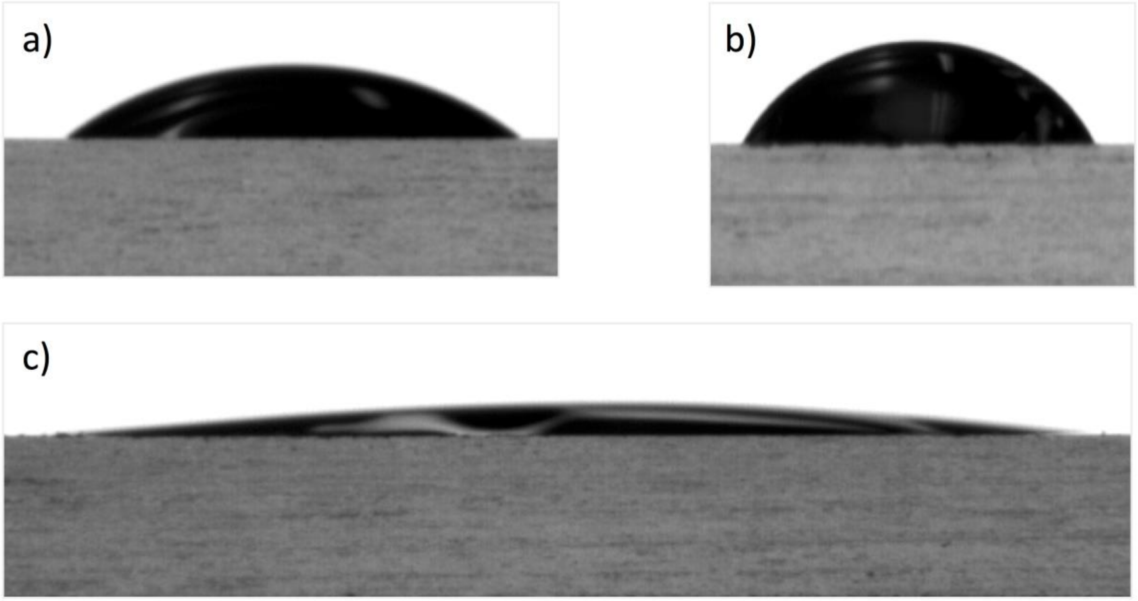

Figure 3.2.2 EMI TFSI ionic liquid on a) untreated glass slide b) hydrophobic coating c) hydrophilic coating

From the contact angles measured and the images above, it is clear that the ionic liquid prefers to wet the hydrophilic surface that has been treated with NaOH the most. One interpretation of this is that there is an increased likelihood of hydrogen bonding between the hydrophilic surface and the ionic liquid compared to the one with the hydrophobic silane coating. In fact, even the untreated glass slide has a smaller contact angle than the silane-treated slide suggesting that the presence of hydroxyl groups on the surface significantly influence the attraction between the liquid and solid surfaces. It is theorized then that the gels made with hydrophilic metal oxides may have a more significant influence on the motion of the ions under a potential difference, i.e. a higher activation energy compared to gels made with hydrophobic species.

3.3. Activation Energy and Ionic Conductivity by Packing Factor

Table 3.3.1 Electrostatic characterization keeping packing factor the same

Species	Room Temp. Conductivity (mS/cm)	Activation Energy (kJ/mol)	Packing Factor (μm^{-1})	Volume % Nanoparticle
Pure EMITFSI	12.2	14.4	0	0
SiO_2 (hydrophilic)	10.0	14.9	10.0	2.1
SiO_2 (hydrophobic)	11.3	14.8	10.0	2.9
Al_2O_3 (hydrophilic)	9.3	15.5	10.0	3.2
Al_2O_3 (hydrophobic)	11.6	14.8	10.0	4.1

E_a values have an error of approximately ± 0.05 kJ/mol. See Appendix D

This table compares the activation energy and ionic conductivities between species keeping the packing factor fixed. The packing factor describes how much surface area of the metal oxide is exposed to the ions of the ionic liquid in a sample, measured in μm^{-1} and was a concept developed solely for the purposes of this thesis investigation.

$$Packing\ Factor\ (\mu m^{-1}) = \frac{Mass\ Nanoparticle\ (kg) \times\ Surface\ Area\left(\frac{m^2}{kg}\right) \times\ 10^{-6}}{((Volume\ of\ Ionic\ Liquid) + (Volume\ of\ Nanoparticle))(m^3)} \tag{E-4}$$

A packing factor of $10\mu m^{-1}$ was decided upon to compare across the metal oxide species as it appropriately balanced the minimum and maximum amounts of all four metal oxide species that could mix with the ionic liquid to form a gel. This packing factor also roughly translates to approximately 1% of the ions of the ionic liquid directly exposed to the surface of the nanoparticles in the gels (See Appendix C for this calculation). This estimate was done neglecting the volume percent contribution by the particles to the system as they were much less than the ionic liquid, shown by the volume percent column in Table 3.5.1, and that the area used by the particles when packing with one another was negligible.

The hypothesis is that the surface of the particles can influence how the ions move due to attractive (or repulsive) forces between the surface and the ions. Specifically, either the hydrophobicity or the metal oxide surface may influence the ionic motion in the gel. Contact angle measurements already show that there is a difference in attraction but it was uncertain whether this could translate to an observable change in the motion of the ions under a potential difference. From the data in Table 3.3.1, the hydrophilic samples have a decreased room temperature ionic conductivity compared to their hydrophobic counterparts. As a reference, the room temperature conductivity of EMI TFSI was measured to be 12.2 mS/cm which agrees with accepted literature values [14]. Compared to the neat ionic liquid conductivity, the decrease in conductivity for these four samples range approximately between 7 and 20%. This is a surprising find since only 1% of the ions in these gel systems, at this packing factor, directly comes into contact with the scaffold surface. It is hypothesized that the hydrophilic surface in the respective gels can slow down or hinder the motion of the ions nearby due to attractive forces being present between the two. Since conductivity is a product of the number of charged species and their speed in the gel, the ionic conductivity is expected to decrease if the scaffold is able to ‘pull’ on the ions nearby.

The metal oxide surface may also exhibit an attractive force towards the ions but it is unclear how much this may be. In hydrophilic gels, the ions are already pulled because of the hydroxyl groups on the scaffold. The metal oxide surface now has a greater chance to effect the ions since more reside more closely. Hydrophobic particles contain significantly less hydroxyl groups and so the metal oxide surface in these gels may not have the opportunity to interface with the ions as much.

The activation energy, E_a, can also be examined in terms of hydrophobicity. A similar trend to the conductivity is seen where the gels that use a hydrophilic scaffold have a higher activation energy, implying that there is a greater hindrance to motion. Theoretically, the activation energy should be a minimum for the neat ionic liquid since there isn’t a scaffold to hinder the motion of ions while a higher activation energy implies an increased barrier to ionic motion. For the gels tested in this investigation, the values ranged between 14 and 16 kJ/mol. This is an important result since polymer gels have previously shown activation energies between 14 and 25 kJ/mol suggesting that nanoparticles may be a preferred scaffold material since it has less of an interaction with the ions.

The activation energies for the alumina samples in Table 3.3.1 differ significantly and it is unclear why. Consistent with the other gels made at the gelation point and by volume percents, the activation energies for the hydrophilic species are always higher than that of the hydrophobic species suggesting that the hydrophilic species have stronger interactions with the ions and can hinder ionic motion (See Appendix A). To get a better idea of the reliability of these numbers, a specific gel recipe was chosen at random and tested several times and the standard deviation was found to be approximately 0.05 kJ/mol (See Appendix D).

3.4. Further E_a Analyses

To better understand the trends in activation energies across the samples fabricated, these values were plotted for the two metal oxides and the two surface chemistries and are shown in the two figures below. They were plotted against the packing factor since this investigation is primarily concerned with the effect, if any, the surface chemistry of metal oxide nanoparticles has on the ions of the ionic liquid. The packing factor is able to provide this yardstick to measure how much surface area of the nanoparticles that the ions are exposed to. A larger packing factor implies that within the gel, the ions interact with more scaffold surface area.

All E_a values have an error of approximately ± 0.05 kJ/mol. See Appendix D

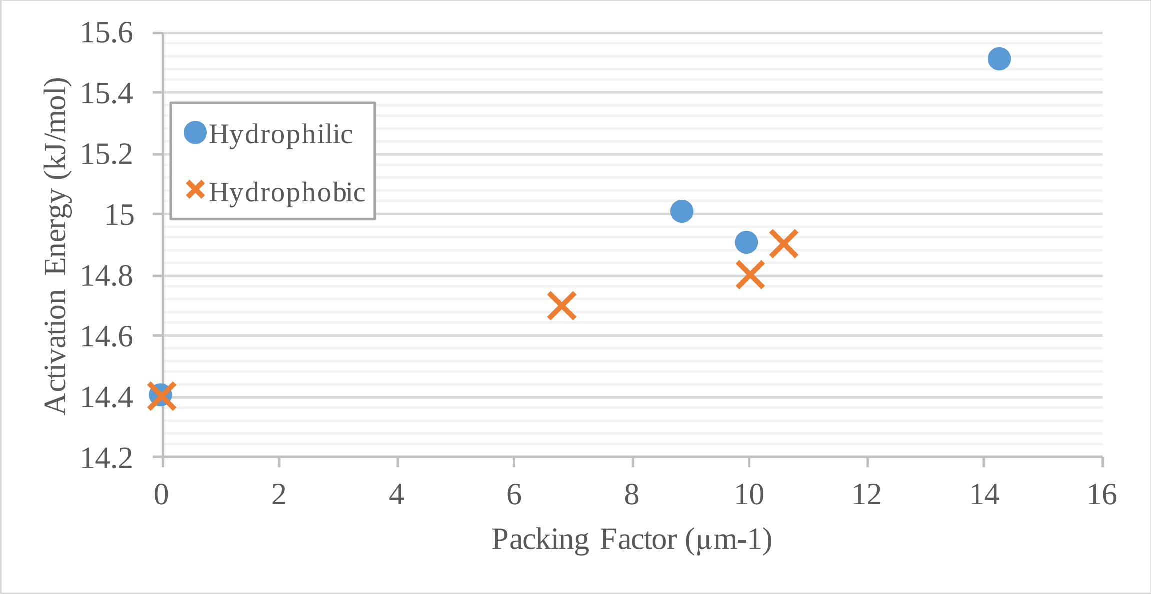

Figure 3.4.1 Activation Energy vs. Packing Factor for gels made up of hydrophilic and hydrophobic silica nanoparticles.

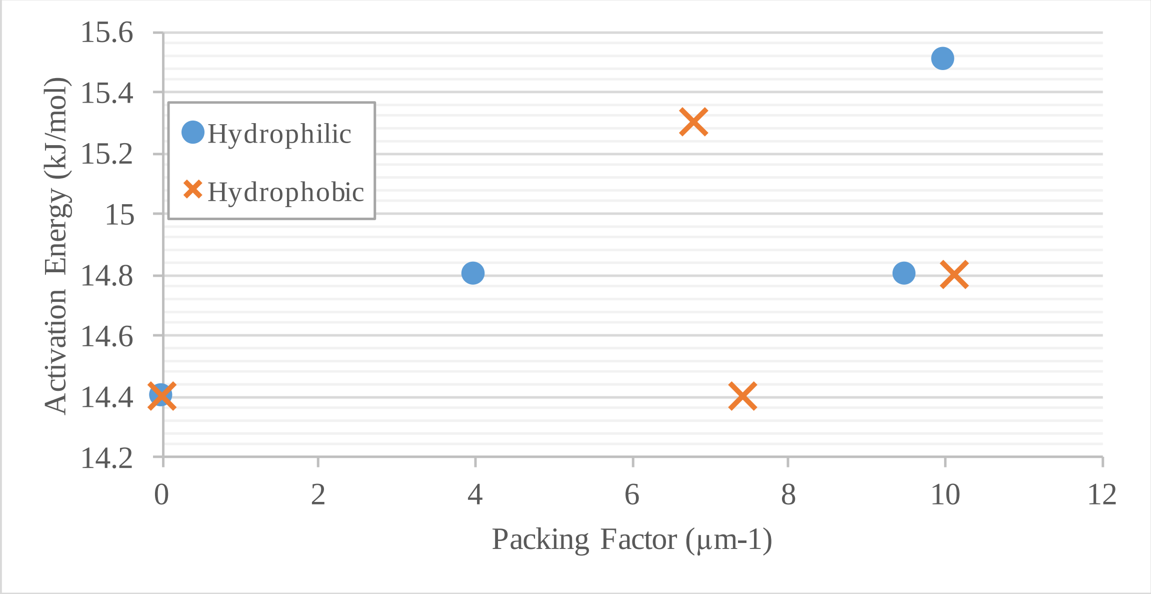

Figure 3.4.2 Activation Energy vs. Packing Factor for gels made up of hydrophilic and hydrophobic alumina nanoparticles

Given the nature of this testing, it was difficult to create enough of the same sample to measure the activation energies multiple times and therefore develop an idea of how repeatable these results were. Ideally, multiple samples of the same composition would be tested and an average value determined.

For the silica graphs, the trend suggests that activation energy increases with increasing amount of nanoparticles (i.e. increasing packing factor). It has been shown previously that the ionic conductivity within the gels decrease with increasing scaffold material for nanoparticle based ionogels [5]. However, this decrease was miniscule. The activation energy was predicted to follow a similar trend and indeed the E_a changes very slightly between all of the gels tested. The slope of the hydrophobic samples in particular is less than that of the hydrophilic ones, which reinforces the idea that there are more ion-scaffold interactions that are inhibitory for the latter. It is hypothesized that it is the ability of the ionic liquid to exhibit hydrogen bonding with the hydrophilic surface of the nanoparticles that presents that additional hindrance that must be overcome under an applied voltage.

Upon examining the alumina gels however, this trend is not observed and it is much more difficult to explain the shape of the hydrophobic graph. With all of the precautions made during testing, it is possible for the activation energy to fluctuate for a number of reasons. Small amounts of moisture from the atmosphere can be absorbed into the ionic liquid. This can decrease the liquid viscosity, increase the conductivity and essentially change the activation energy. To minimize this error, samples were tested as soon as possible after their synthesis and the nanoparticle powder and ionic liquid vials were kept in cool, dry places when not in use. Most likely is that the hydrophobic alumina sample at a packing factor of 7µm^{-1} was not set up properly. The electrodes of the potentiostat can introduce error since they are inserted anew each time. It is assumed that their approximate placement within the sample, i.e. their distance from each other, is kept the same so that conductivity values do not fluctuate significantly between trials. Examination of the hydrophilic sample activation energies once more suggest that while it does increase with scaffold concentration, the magnitude is not significant due to the small surface area exposure and volume taken up by the scaffold.

4. Conclusions

Ionogels were successfully synthesized using hydrophilic and hydrophobic silica and for the first time, alumina nanoparticles with the hydrophobic ionic liquid EMI TFSI. Despite the hydrophobic nature of the ionic liquid as reported in literature, there is a greater affinity by the ionic liquid for the hydrophilic surfaces of the metal oxide nanoparticles. It is hypothesized that hydrogen bonding is possible between the ions of the liquid and the hydrophilic surface of the nanoparticles and this influences the behavior of the gel in several ways.

The ionogels are formed due to a colloidal 3D network that expands in fractals throughout the liquid volume. The particles that form this network are able to bond with each other due to attractive Van der Waal forces and in the case of hydrophilic particles, hydrogen bonding contributes to interparticle bonding. When gels fabricated using hydrophilic particles are agitated, they assume a liquid state that appears to flow. However, after a short period of time, the gelatinous state seen previously returns and this has been explained by the temporary disruption of the interparticle network by the breaking of the hydrogen bonds. Particle size also determined the formation of any sort of gel material as gels based on titanium dioxide could not be synthesized due to the larger primary particle size.

Under a potential difference, the ions of the ionic liquid within the gel are also affected by the nature of the particle surface. Activation energy was measured in this investigation as it is a measure of the hindrance experienced by ions in the gel while they are in motion. The trend observed was that for all the gels, the activation energy did not significantly increase with an increasing amount of particle scaffold, suggesting that ionogels based on this colloidal system are very effective in preserving the electrostatic properties of the neat ionic liquid. Gels based on hydrophilic particles appear to have slightly higher activation energies than those based around hydrophobic ones. The ionic conductivity also mirrors this trend in that it decreases with the hydrophilic species compared to the hydrophobic gels. It is hypothesized that since the particle surfaces for hydrophilic nanoparticles can form hydrogen bonds with the ions of the ionic liquid, there is an additional resistance to the movement of ions within the gel and therefore, the increase in activation energy is observed.

Nanoparticles as a scaffold material for ionogels are unique as they allow a simple fabrication process, require the least concentration (2-3% by weight) to form a gel compared to other scaffolds like polymers, are thermally stable and are readily available and inexpensive. This thesis attempts to further the understanding of the electrostatic behavior within novel solid electrolyte materials intended for use in energy storage devices so that more informed decisions can be made about the selection of scaffold and ionic liquid material. The focus was primarily on the chemical interactions between the nanoparticle surface and the ions of the ionic liquid and examining the effect on electrostatic behavior, if any, due to the nanoparticle identity and the surface hydrophobicity.

5. Future Work

For this investigation, the activation energy of different general samples were examined. This value for all of the gels tested fluctuated between 14 and 16 kJ/mol and it is likely that there was significant source of error associated with these values. For future experiments involving the measurement of activation energy, it is recommended that the same gel composition be tested several times to get a better average value. Previous groups have also reported synthesizing metal oxide nanoparticles and being able to tune their particle sizes. It would be useful to fabricate ionogels using particles of the same size but different metal oxide identity.

Although it is understood that the metal oxides contain hydroxyl groups on their surfaces, their concentration has not yet been defined. IR spectroscopy can be used to quantify the number of O-H bonds present in both hydrophilic and hydrophobic particles and give a better sense of their significance to electrostatic results.

To better characterize the particulate network in the gel samples, it may be instructive to examine them using transmission electron microscopy (TEM) as has been done previously by Ueno et al [5]. Finally, the ionic liquid used in this investigation can also be substituted for another and the type of attraction between it and hydrophobic or hydrophilic glass slides or nanoparticles can be further examined.

6. Appendix

6.1. Appendix A

Table 6.1.1 Activation Energy Measurements at Gelation Points

Species	Activation Energy (kJ/mol)	Weight % Nanoparticle	Volume % Nanoparticle	Packing Factor (μm^{-1})
Pure EMITFSI	14.4	0	0	0
SiO_2 (hydrophilic)	15.0	2.7	1.9	8.9
SiO_2 (hydrophobic)	14.7	2.8	2.0	6.8
Al_2O_3 (hydrophilic)	14.8	2.7	1.3	4.0
Al_2O_3 (hydrophobic)	15.3	4.6	2.8	6.8

E_a values have an error of approximately ± 0.05 kJ/mol. See Appendix D

The gel points, i.e. the minimum amount of nanoparticle species required to form a gel, were first investigated. In general, gels based on hydrophobic metal oxides require more particles by mass to make a gel compared to that of hydrophilic ones. This may be explained by the additional interparticle hydrogen bonding that is possible between hydrophilic metal oxide species as explored in the previous section. The presence of more interparticle bonding suggests that it is easier to construct the characteristic particulate network necessary for a gel. It should be noted that the densities of the two alumina species are significantly different and account for the significant difference in volume fraction seen.

Table 6.1.2 Activation Energy Measurements at 3% Volume Fractions

Species	**Activation Energy (kJ/mol)**	**Weight % Nanoparticle**	**Volume % Nanoparticle**	**Packing Factor (μm^{-1})**
Pure EMITFSI	14.4	0	0	0
SiO_2 (hydrophilic)	15.5	4.3	3.0	14.3
SiO_2 (hydrophobic)	14.9	4.3	3.0	10.6
Al_2O_3 (hydrophilic)	14.7	6.2	3.00	9.5
Al_2O_3 (hydrophobic)	14.4	5.0	3.0	7.4

E_a values have an error of approximately ± 0.05 kJ/mol. See Appendix D

This table compares the activation energy based on a fixed volume percent of nanoparticle species within the ionogel. One theory is that the ionic transport in the gel is physically obstructed by the presence of the nanoparticle network and cannot move as quickly as it can in the neat liquid. Keeping the volume percent the same across the gel samples and measuring a difference between the activation energies suggest that the volume of the scaffold cannot account entirely for the nature of the ionic motion within the gel.

6.2. Appendix B

$$Approximate\ Molecular\ Area\ of\ EMI\ TFSI = 0.56\ nm^2$$

$$Density\ of\ EMI\ TFSI = 1.52\ g/cm^3$$

$$Molecular\ Weight\ of\ EMI\ TFSI = 391.91\ g/mol$$

A packing factor of 10 μm^{-1} implies that the volume of ionic liquid that comes into contact with 1 μm^2 on a particle surface is $0.1\mu m^3$ since

$$Packing\ Factor = \frac{Surface\ Area\ of\ Nanoparticle}{Volume\ of\ IL} = \frac{1\mu m^2}{0.1\mu m^3} = 10\mu m^{-1}$$

assuming that the volume of nanoparticle material to ionic liquid is insignificant.

The image below shows this $0.1\mu m^3$ ionic liquid (orange) on the surface of $1\mu m^2$ area of nanoparticle material.

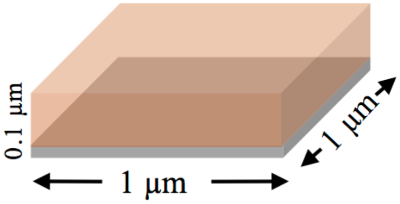

Not to scale

First, calculating the number of IL molecules in this volume gives

$$\#\ of\ IL\ molecules = 0.1\ \mu m^3 \left(\frac{cm}{10^4 \mu m}\right)^3 \left(\frac{1.52 g\ IL}{cm^3}\right)\left(\frac{mol}{391.91\ g\ IL}\right)\left(\frac{6.022 \times 10^{23}\ molecules}{mol}\right)$$

$$= 2.34 \times 10^8\ IL\ molecules$$

Second, calculating the number of molecules on the surface of the nanoparticle material gives

$$\#\ of\ IL\ molecules\ on\ nanoparticle\ surface = 1\ \mu m^2 \left(\frac{10^3 nm}{\mu m}\right)^2 \left(\frac{IL\ molecules}{0.56\ nm^2}\right)$$

$$= 1.79 \times 10^6\ IL\ molecules$$

Therefore, the fraction of IL molecules in the gel that is theoretically interfacing with the surface of the scaffold as a percentage is

$$\left(\frac{1.79 \times 10^6}{2.34 \times 10^8}\right) \times 100\% = \mathbf{0.76}\%$$

6.3. Appendix C

Scanning Electron Microscopy (SEM) images of the six different species of nanoparticle species examined in this study at a magnification of 200,000 times. Images were taken at the Center for Nanoscale Systems at Harvard University.

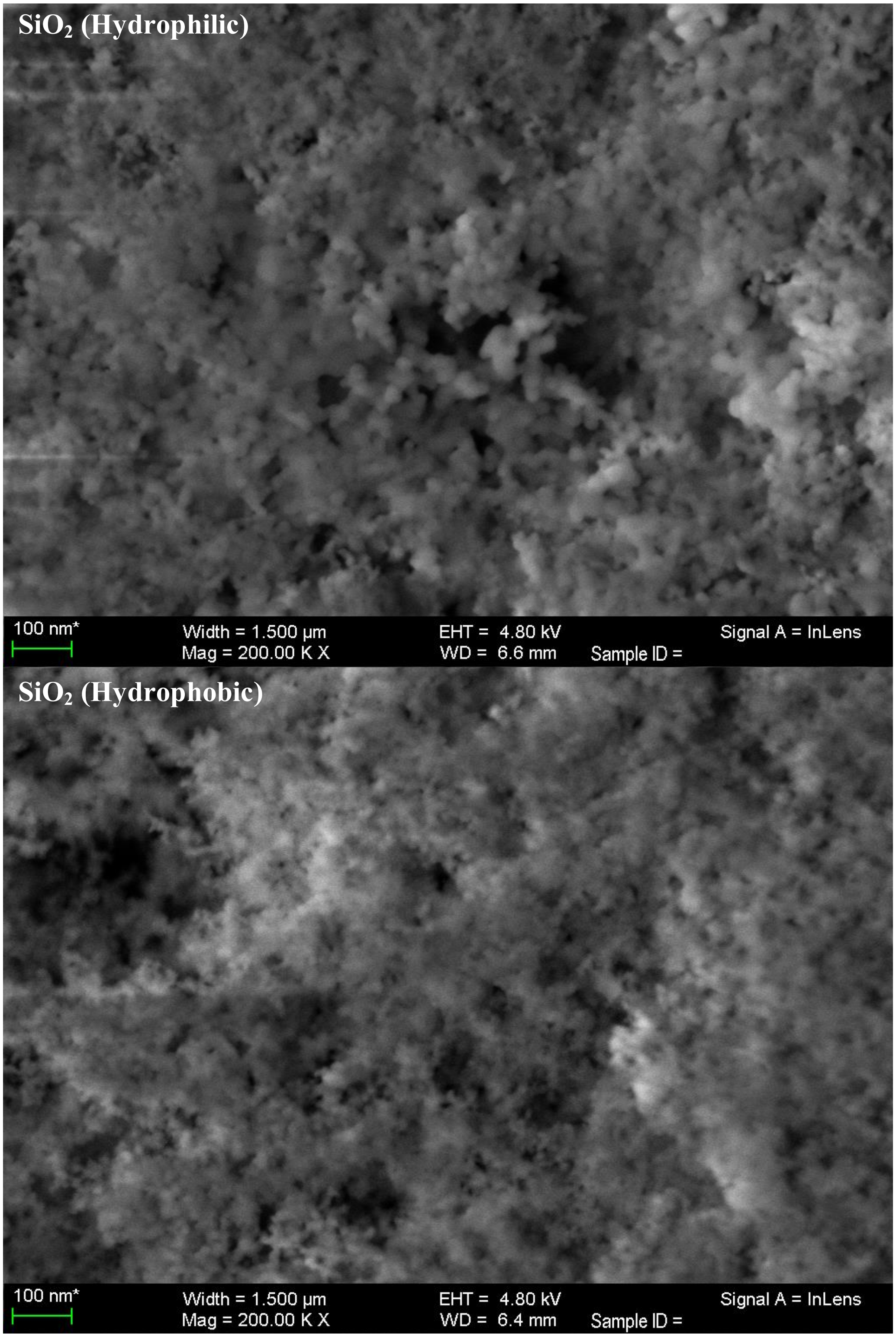

Figure 6.3.1 SEM Images of hydrophilic and hydrophobic silica nanoparticles at 200K magnification

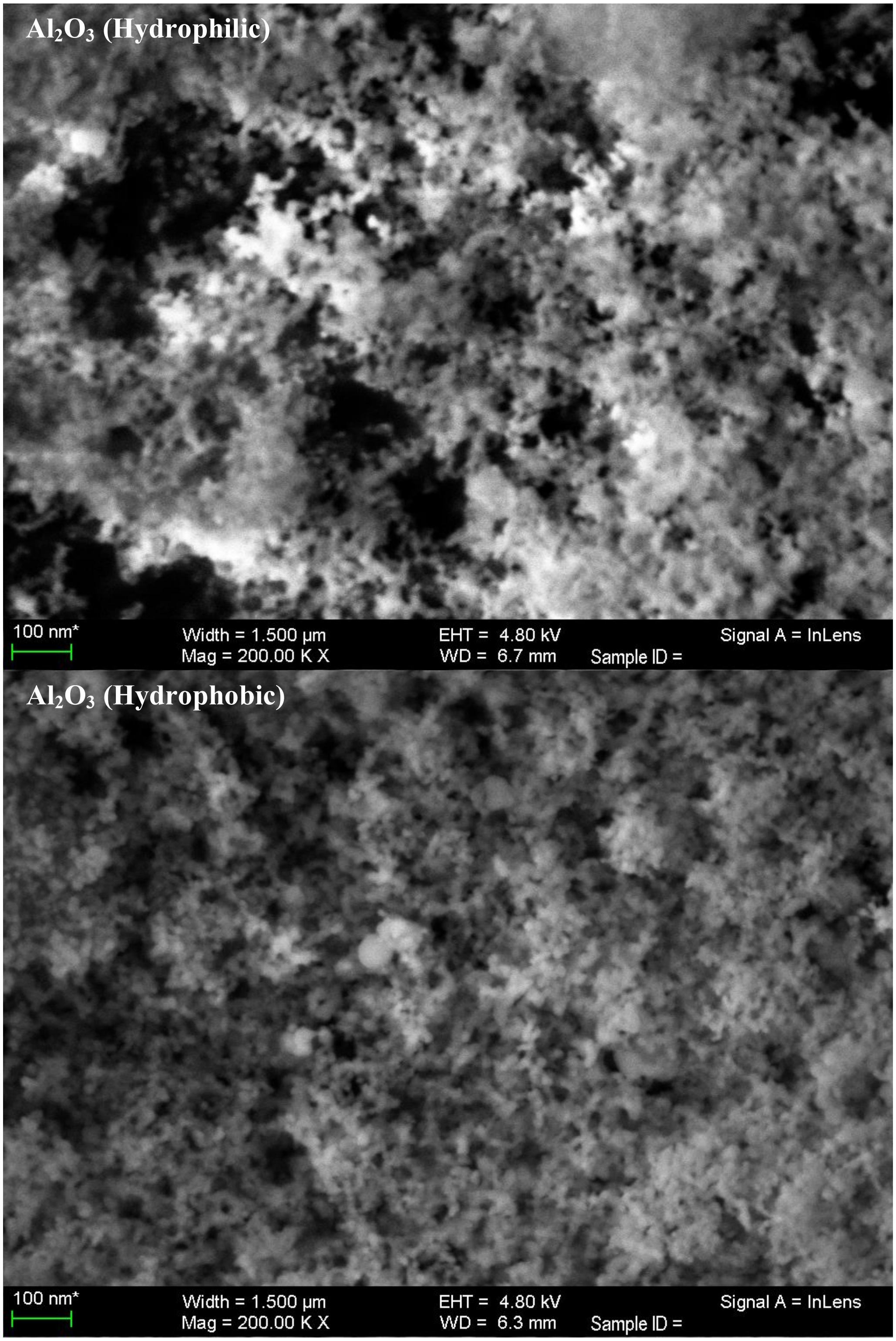

Figure 6.3.2 SEM Images of hydrophilic and hydrophobic alumina nanoparticles at 200K magnification

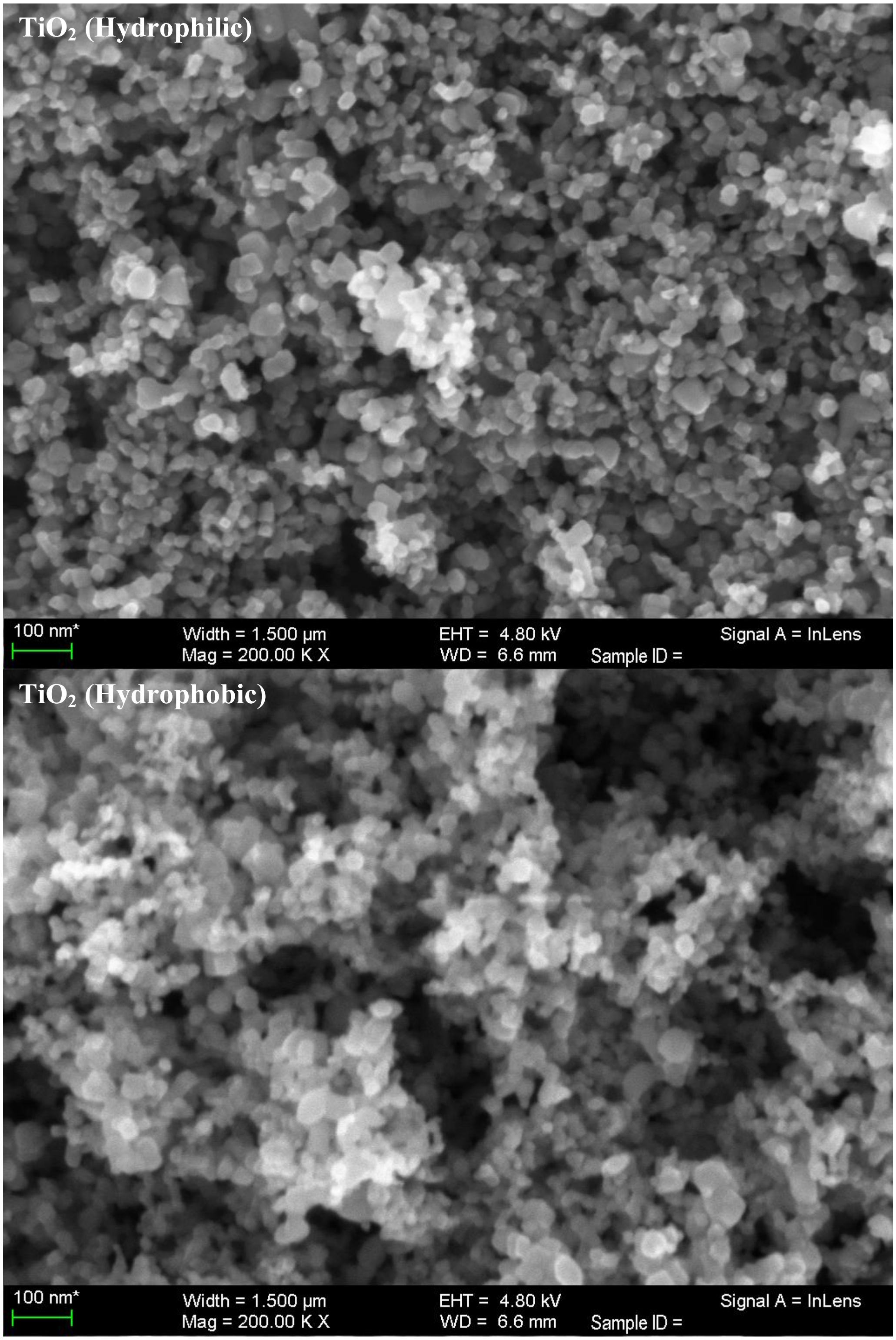

Figure 6.3.3 SEM Images of hydrophilic and hydrophobic titania nanoparticles at 200K magnification

6.4. Appendix D

To have better confidence in the activation energy numbers obtained, the E_a of a sample with a predetermined composition was investigated over three trials. The standard deviation of the three trials and the original trial (hydrophilic alumina based on a 3 volume percent recipe) was determined to be approximately 0.05.

Table 6.4.1 Repeatability Tests of Activation Energy Results

Trial (3% Volume Al_2O_3[I])	**Activation Energy (kJ/mol)**
Original Run	14.7
Trial 1	14.7
Trial 2	14.6
Trial 3	14.7
Standard Deviation	0.05

7. References

[1] Armand, M., and J.-M. Tarascon. "Issues and Challenges Facing Rechargeable Lithium Batteries." *Nature* 414.6861 (2001): 359.*Canadian Periodicals Index Quarterly*.

[2] Vioux, André, Lydie Viau, Sabrina Volland, and Jean Le Bideau. "Use of Ionic Liquids in Sol-gel; Ionogels and Applications." *Comptes Rendus Chimie.* 13.1-2 (2010): 242-55.

[3] Horowitz, Ariel I., and Matthew J. Panzer. "High-performance, Mechanically Compliant Silica-based Ionogels for Electrical Energy Storage Applications." *Journal of Materials Chemistry* 22.32 (2012): 16534.

[4] Ueno, Kazuhide, Satoru Imaizumi, Kenji Hata, and Masayoshi Watanabe. "Colloidal Interaction in Ionic Liquids: Effects of Ionic Structures and Surface Chemistry on Rheology of Silica Colloidal Dispersions." *Langmuir* 25.2 (2009): 825-31.

[5] Ueno, Kazuhide and Masayoshi Watanabe. “Silica Colloidal Suspensions in Ionic Liquids: Colloidal Stability and Fabrication of Ion Gels on the basis of Colloidal Self-Assembly.” *Ionic Liquids: From Knowledge to Application.* (2010): 199-210.

[6] Wittmar, Alexandra, Martyna Gajda, Devendraprakash Gautam, Udo Dörfler, Markus Winterer, and Mathias Ulbricht. "Influence of the Cation Alkyl Chain Length of Imidazolium-based Room Temperature Ionic Liquids on the Dispersibility of TiO2 Nanopowders." Journal of Nanoparticle Research 15.3 (2013): 1-12

[7] Susan, Md. Abu Bin Hasan, Taketo Kaneko, Akihiro Noda, and Masayoshi Watanabe. "Ion Gels Prepared by in Situ Radical Polymerization of Vinyl Monomers in an Ionic Liquid and Their Characterization as Polymer Electrolytes." *Journal of the American Chemical Society* 127.13 (2005): 4976-983.

[8] Horowitz, Ariel I., and Matthew J. Panzer. "Poly(dimethylsiloxane)-Supported Ionogels with a High Ionic Liquid Loading," *J. Angew. Chem. Int. Ed.* 53, (2014): 9780-9783.

[9] Wong, Jessica X. H., and Hua-Zhong Yu. "Preparation of Transparent Superhydrophobic Glass Slides: Demonstration of Surface Chemistry Characteristics." *Journal of Chemical Education* 90.9 (2013): 1203-206.

[10] Largeot, Celine, Cristelle Portet, John Chmiola, Pierre-Louis Taberna, Yury Gogotsi, and Patrice Simon. "Relation between the Ion Size and Pore Size

for an Electric Double-Layer Capacitor." Journal of the American Chemical Society 130.9 (2008): 2730-731.

[11] "Influence of Ionic Liquid Selection on the Properties of Poly(Ethylene Glycol) Diacrylate-Supported Ionogels as Solid Electrolytes," Visentin, A. F.; Alimena, S.; Panzer, M. J. *ChemElectroChem* 2014, *1*, 718-721.

[12] Ueno, Kazuhide, Kenji Hata, Toru Katakabe, Masashi Kondoh, and Masayoshi Watanabe. "Nanocomposite Ion Gels Based on Silica Nanoparticles and an Ionic Liquid: Ionic Transport, Viscoelastic Properties, and Microstructure." *The Journal of Physical Chemistry B* 112.30 (2008): 9013-019.

[13] Yang, Hong, Chengzhong Yu, Qunliang Song, Yongyao Xia, Fuyou Li, Zhigang Chen, Xianghong Li, Tao Yi, and Chunhui Huang. "High-Temperature and Long-Term Stable Solid-State Electrolyte for Dye-Sensitized Solar Cells by Self-assembly." *Chemistry of Materials* 18.22 (2006): 5173-177.

[14] Zhang, Suojiang, Ning Sun, Xuezhong He, Xingmei Lu, and Xiangping Zhang. "Physical Properties of Ionic Liquids: Database and Evaluation." *Journal of Physical and Chemical Reference Data* 35.4 (2006): 1475.